

# Analysis and Reduction of Floating Diffusion Capacitance Components of CMOS Image Sensor for Photon-Countable Sensitivity

Fumiaki Kusuhara, Shunichi Wakashima, Satoshi Nasuno, Rihito Kuroda and Shigetoshi Sugawa  
 Graduate School of Engineering, Tohoku University  
 6-6-11-811, Aza-Aoba, Aramaki, Aoba-ku, Sendai, Miyagi, Japan 980-8579  
 TEL: +81-22-795-4833, FAX: +81-22-795-4834, Email address: kusuhara@dc.tohoku.ac.jp

## ABSTRACT

In this paper, we describe an analysis methodology of components of floating diffusion (FD) capacitance ( $C_{FD}$ ) and propose  $C_{FD}$  reduction methods for photon-countable sensitivity. We extracted each  $C_{FD}$  component using developed test patterns and confirmed that the sum of them agrees well with the measurement result of  $C_{FD}$  in sensor.  $C_{FD}$  reduction method based on the result of analysis was applied to FD and pixel source follower (SF). Its effectiveness was verified by the fabricated CMOS image sensor chip exhibiting conversion gain (CG) of  $243\mu\text{V}/e^-$  ( $C_{FD}$  of 0.66fF).

## INTRODUCTION

Image sensors with high signal-to-noise ratio (SNR) are required in various areas; information equipment including smartphone, industrial measurement, medical, in-vehicle equipment, security, etc. To achieve the high SNR, some approaches, electron multiplication [1], column amplifier and ADC [2-3], increasing CG at FD [4-5], have been reported.

Recently, many researches with regard to high SNR that allows photon counting have been carried out actively. It is necessary to reduce the input referred noise to  $0.20e^-_{\text{rms}}$  for achieving the photon-countable sensitivity [6-7].

In the CMOS image sensor, increasing the gain at input stage of the readout circuit is the most valid method to reduce the input referred noise. In that sense, increasing CG is the most effective way. Therefore, analysis and reduction of the  $C_{FD}$  components are extremely important. It should be noted that satisfying both high CG and high full well capacity (FWC) is also important.

In this paper, an analysis methodology of  $C_{FD}$  using test element group (TEG) is described at first. Then,  $C_{FD}$  reduction method with device structure is proposed. Finally, the measurement results of image sensor chip we designed and fabricated are discussed.

## THE ANALYSIS OF $C_{FD}$ COMPONENTS

$C_{FD}$  consists of p-n junction capacitance, gate overlap capacitance, and metal capacitance. Figure 1 shows an example of general pixel layout and its cross-sectional views and table 1 summarizes the detailed components of  $C_{FD}$ .

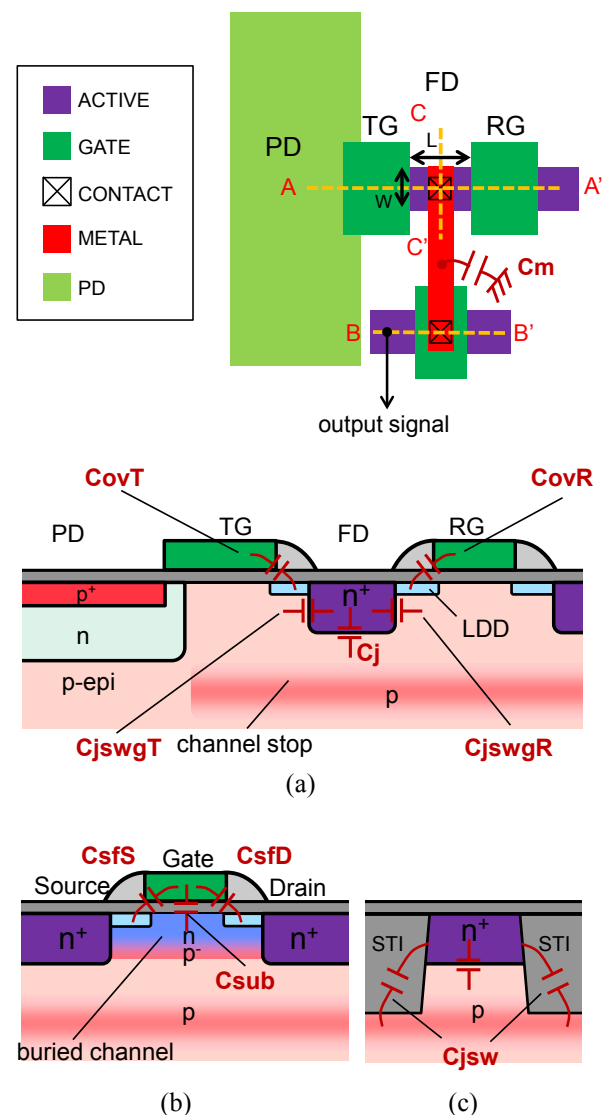


Fig. 1. Example of general pixel layout (upper figure) and cross-sectional views of (a) A-A', (b) B-B', (c) C-C'.  $C_{FD}$  consists of p-n junction capacitance, gate overlap capacitance, and metal capacitance.

Table 1. The detailed components of  $C_{FD}$ .

Main components of $C_{FD}$	Components of $C_{FD}$	Explanation
Gate overlap capacitance	$(1-G_{SF}) \times C_{sfS}$	gate overlap capacitance between gate and source at pixel SF with mirror effect
	$C_{sfD}$ & $C_{sub}$	gate overlap capacitance between gate and drain at pixel SF and capacitance between gate and substrate at pixel SF
	$C_{ovR}$	gate overlap capacitance between FD and RG
	$C_{ovT}$	gate overlap capacitance between FD and TG
P-n junction capacitance	$C_{jsw}$	p-n junction capacitance between FD and p-epi under STI
	$C_{jswgR}$	p-n junction capacitance between FD and p-epi under RG
	$C_{jswgT}$	p-n junction capacitance between FD and p-epi under TG
	$C_j$	p-n junction capacitance between FD and p-epi under FD
Metal capacitance	$C_m$	metal capacitance

Figure 2 shows the conceptual diagrams of TEG used for extracting the components of  $C_{FD}$  in this work. Table 2 summarizes the detail of the TEG. The area of developed TEG is large enough to measure C-V characteristics accurately by existing impedance analyzers. Measuring the C-V curve of two TEGs, type A and B, and normalizing to the real size of FD in sensor, we can extract both p-n junction capacitance components,  $C_j$  and  $C_{jsw}$ . Additionally, measuring type C and using the data of  $C_j$  and  $C_{jsw}$  extracted from type A and B, we can obtain p-n junction capacitances,  $C_{jswgT}$  and  $C_{jswgR}$ , and gate overlap capacitance,  $C_{ovT}$ ,  $C_{ovR}$ ,  $C_{sfD}$ , and  $C_{sfS}$ . Thus, using linear calculations with various areas and lengths of STI and gate, we can extract all of the  $C_{FD}$  components listed in Table 1.

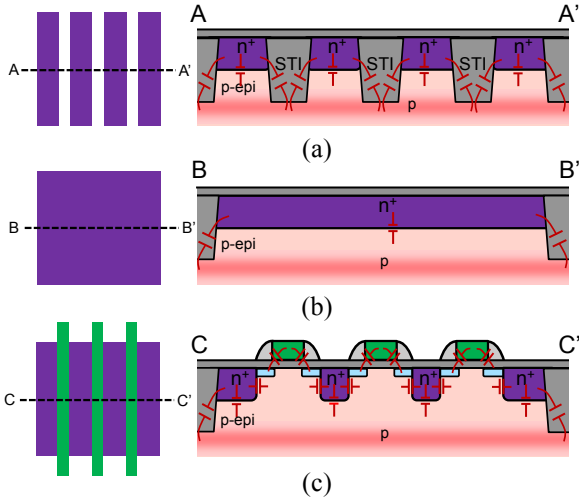


Fig. 2. Measurement TEG for (a) type A (b) type B (c) type C

Table 2. The detailed of TEG patterns.

TEG patterns	Area [ $\mu\text{m}^2$ ]	Length of STI [ $\mu\text{m}$ ]	Length of gate [ $\mu\text{m}$ ]
type A	1254	2552	—
type B	3648	242	—
type C	2337	200	2394

Measurement results of C-V characteristics about the components of  $C_{FD}$  assuming the image sensor with FD size (W/L) of  $0.34\mu\text{m}/0.44\mu\text{m}$  are shown in Figure 3. The capacitances are almost constant for  $V_{FD}$  of 2.0-3.0V, where this voltage range is used for the actual image sensor.

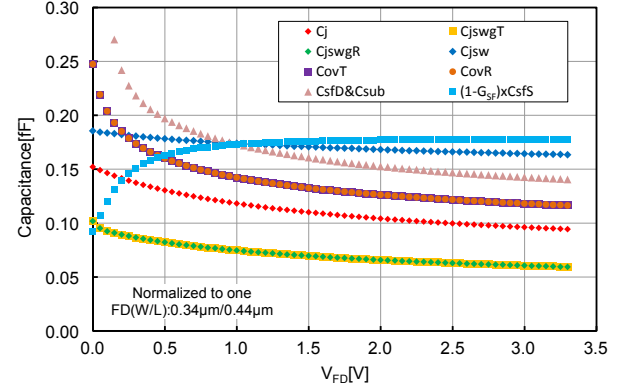


Fig. 3. Measurement results of C-V characteristics.

In Figure 4, the measurement result of  $C_{FD}$  in conventional CMOS image sensor is compared with TEG. Here, FD size of the sensor chip was  $0.34\mu\text{m}/0.44\mu\text{m}$  and pixel SF size was  $0.45\mu\text{m}/0.50\mu\text{m}$ . Pixel SF gain was 0.827 that was the measurement result of the sensor. Metal capacitance was estimated by the layout of the sensor. It is clear that the sum of  $C_{FD}$  components agrees well with the measurement result of  $C_{FD}$  in sensor. Also, gate overlap capacitance accounts for the highest percentage of  $C_{FD}$ , and p-n junction capacitance is following.

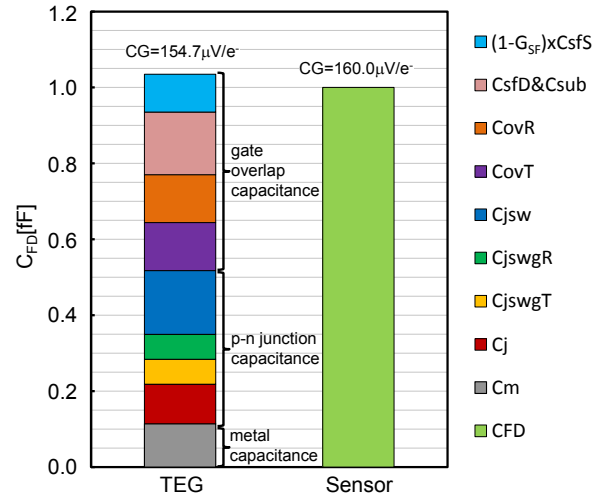


Fig. 4. Measurement results of  $C_{FD}$  in TEG and sensor

## DEVICE STRUCTURE FOR REDUCING $C_{FD}$

Based on the results so far, we propose a device structure for reducing  $C_{FD}$ . Figure 5 shows the cross-sectional views of the small  $C_{FD}$  device structure. In this structure, omitting the implantation process of lightly doped drain (LDD) at FD and drain of pixel SF,  $n^+$  diffusion layers with offset are formed by the self-aligned process [4]. By this means, gate overlap capacitance decreases. Also, using low dose at FD and drain of pixel SF and omitting the implantation process of channel stop under FD, depletion layer width increases. It contributes to the reduction of p-n junction capacitance. Additionally, applying low implant energy to FD and drain of pixel SF to make the p-n junction shallow. In consequence, the surface area of p-n junction reduces and this leads to the farther decrease of p-n junction capacitance and gate overlap capacitance. We revealed the implantation condition with no problem about charge transfer and hot electron. Regarding the pixel SF, the reason for omitting the implantation process of LDD and applying low dose and implant energy only to drain side is that source side is affected by a mirror effect which multiplies  $C_{sf}$  by  $(1-G_{SF})$ , where  $G_{SF}$  is the gain of pixel SF. It is the purpose of this asymmetric pixel SF structure to suppress an increase of resistance and the degradation of the pixel SF gain. It is important to note that these processes were applied to FD and pixel SF.

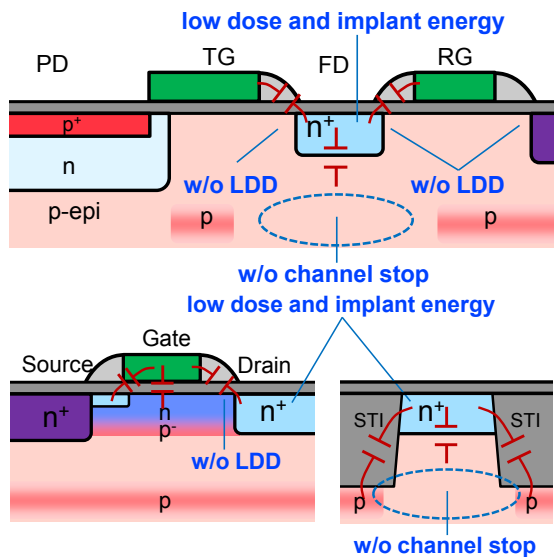


Fig. 5. Cross-sectional views of the proposed small  $C_{FD}$  device structure

## CHIP FABRICATION AND RESULTS

We designed and fabricated image sensor chip with the device structure reflecting the proposed reducing method. Figure 6 shows the  $C_{FD}$  components and the

net doping distribution of (a) conventional FD ( $n^+$  with LDD), (b)  $n^+$  without LDD, (c) low dose and implant energy  $n^+$  without LDD and channel stop, (d) fine processing technology in (c). The values of  $C_{FD}$ s were obtained by measurements and the device simulations and the net doping distributions were calculated by the device simulation. We achieved a CMOS image sensor with high CG over  $240\mu V/e^-$  in the case of (c) because of low dose and implant energy  $n^+$  without LDD in FD and drain of pixel SF and no channel stop under FD. The lines on the net doping distribution illustrate the edges of the depletion layers. Though, this time, we used  $0.18\mu m$  CMOS process technology, if we use more miniaturized process technology, for example, supposing FD size is  $0.12\mu m/0.25\mu m$  and pixel SF size is  $0.20\mu m/0.52\mu m$ , and apply the proposed method, we can estimate  $C_{FD}$  of  $0.38fF$  and CG of  $420\mu V/e^-$ .

Figure 7 shows the fabricated image sensor chip employing the device structure reflecting the proposed  $C_{FD}$  reducing method. This chip was fabricated using  $0.18\mu m$  1-Poly 5-Metal CMOS process technology with pinned PD. FD is the minimum size in this process,  $0.34\mu m/0.44\mu m$ , and pixel SF size is  $0.34\mu m/0.52\mu m$ . Figure 8 shows the captured image by using the CMOS image sensor with CG of  $243\mu V/e^-$  ( $C_{FD}$  of  $0.66fF$ ) at room temperature with the average number of signal electrons, (a)  $\sim 3e^-$ , (b)  $\sim 10e^-$ , (c)  $\sim 30e^-$ . Input referred noise of this sensor is  $0.46e^-_{rms}$  [8]. Combining the proposed small  $C_{FD}$  pixel with lateral overflow integration capacitor (LOFIC) technology [8-9], we can achieve both almost photon-countable sensitivity and high FWC with a single exposure.

## CONCLUSION

The components of  $C_{FD}$  extracted experimentally were demonstrated, and we proposed the very small  $C_{FD}$  structure with low concentration and shallow FD junction without LDD. We designed and fabricated the image sensor chip with the device structure reflecting the proposed  $C_{FD}$  reducing method, and it exhibited  $C_{FD}$  of  $0.66fF$  and CG of  $243\mu V/e^-$ .

## REFERENCES

- [1] K. Tanioka, et al, IEEE Electron Device Lett., 8, 9, pp392-394, 1987.
- [2] B. Fowler, et al, International Image Sensor Workshop, 2009.
- [3] Y. Nitta, et al, Int. Solid-State Circuits Conf., Digest Tech, pp500-501, 2006.
- [4] S. Adachi, et al, Symp. VLSI Circ., Digest Tech, pp142-143, 2007.
- [5] J. Ma, et al, International Electron Device Meeting, 10.1.1-10.1.4, 2014.
- [6] J. R. Janesick, Photon Transfer  $DN \rightarrow \lambda$ , 2007.
- [7] E. Fossum, International Image Sensor Workshop, pp.313-316, 2013.
- [8] S. Wakashima, et al, Symp. VLSI Circ., Digest Tech, to be published 2015.
- [9] S. Sugawa, et al, Int. Solid-State Circuits Conf., Digest Tech, pp.352-353, 603, 2005.

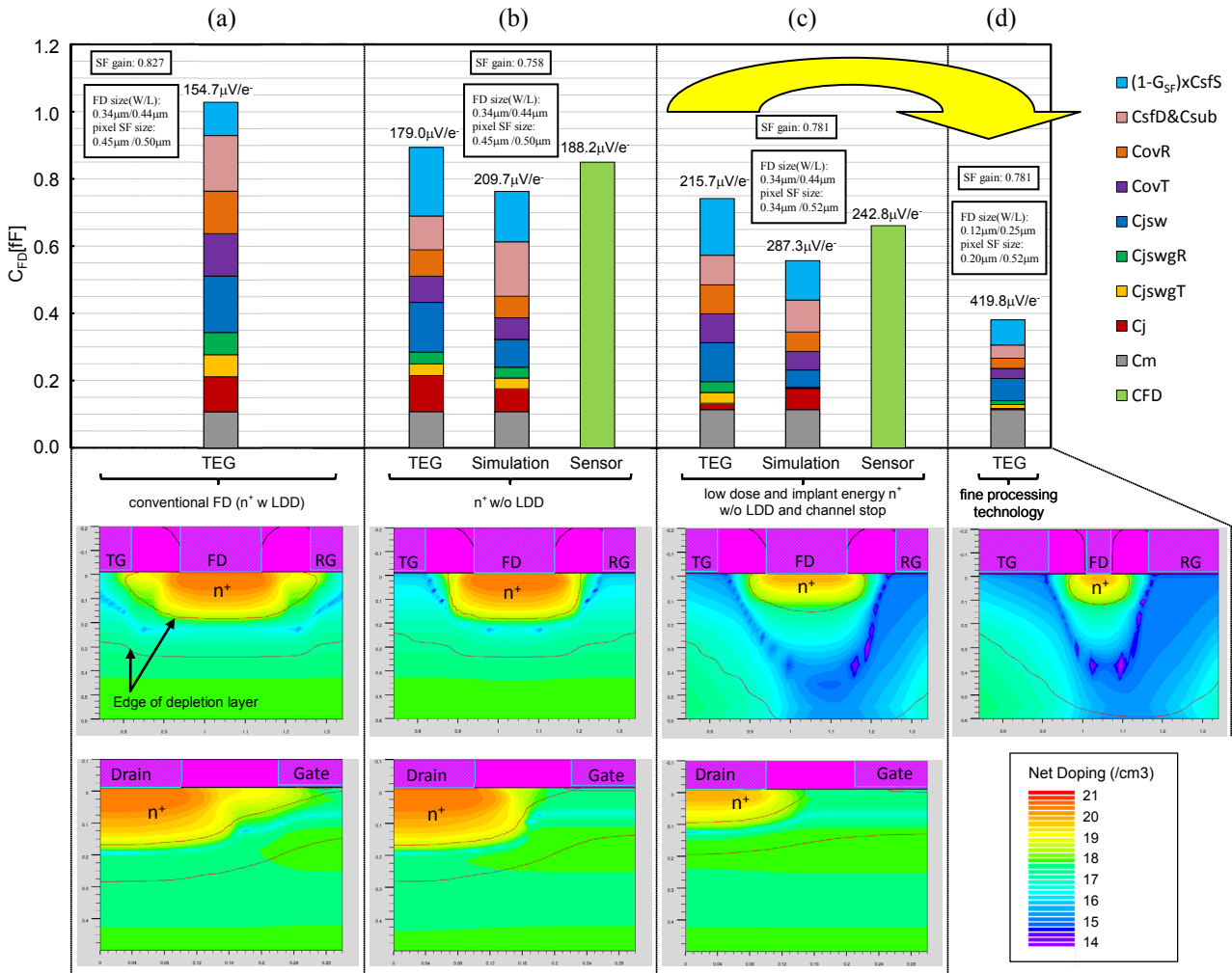


Fig. 6. Measurement and simulation results of  $C_{FD}$  in pixel transistors and simulation results of net doping distribution.

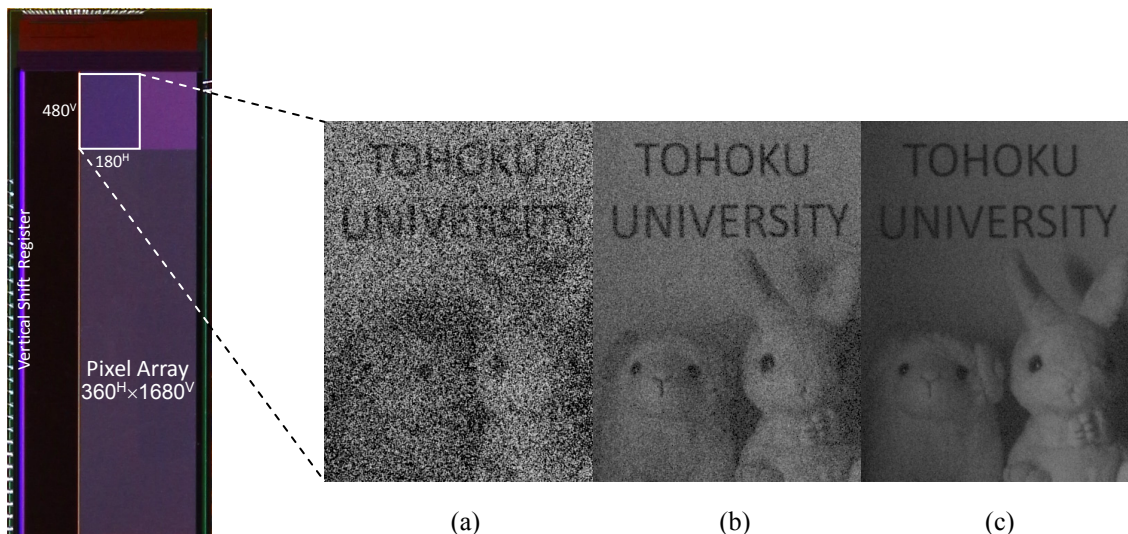


Fig. 7. Fabricated CMOS image sensor chip micrograph.

Fig. 8. Captured image at room temperature with the average number of signal electrons, (a)  $\sim 3e^-$ , (b)  $\sim 10e^-$ , and (c)  $\sim 30e^-$ , with  $F\# = 4.0$ . The number of pixels is  $180^H \times 480^V$ .